First laboratory validation of vibration filtering with LQG control law for Adaptive Optics

Cyril Petit, Jean-Marc Conan, Caroline Kulcsár, Henri-Francois Raynaud, Thierry Fusco

First laboratory validation of vibration filtering with LQG control law for Adaptive Optics

Cyril Petit[1*], Jean-Marc Conan[1], Caroline Kulcsár[2], Henri-Francois Raynaud[2], Thierry Fusco[1]

[1] *Office National d'Etudes et de Recherches Aérospatiales, BP 72, 92322 Châtillon, France*
[2] *Université Paris 13, Institut Galilée, L2TI, 93430 Villetaneuse, France*
cyril.petit@onera.fr

Abstract: We present a first experimental validation of vibration filtering with a Linear Quadratic Gaussian (LQG) control law in Adaptive Optics (AO). A quasi-pure mechanical vibration is generated on a classic AO bench and filtered by the control law, leading to an improvement of the Strehl Ratio and image stability. Vibration filtering may be applied to any AO system, but these results are of particular interest for eXtrem AO, and for instance for the SPHERE AO design, where high performance is required.

OCIS codes: (010.1080) Adaptive optics; (100.3190) Inverse problems

References and links

1. G. Rousset, F. Lacombe, P. Puget, N. Hubin, E. Gendron, T. Fusco, R. Arsenault, J. Charton, P. Gigan, P. Kern, A.-M. Lagrange, P.-Y. Madec, D. Mouillet, D. Rabaud, P. Rabou, E. Stadler and G. Zins, "NAOS, the first AO system of the VLT: on sky performance," in *Adaptive Optical System Technology II*, Bellingham, Proc. SPIE **4839**, 140–149, (2002).
2. Y. Clénet, M.E. Kasper, N. Ageorges, C. Lidman, T. Fusco, O. Marco, M. Hartung, D. Mouillet, B. Koehler, G. Rousset and N. Hubin, "NACO performance: status after 2 years of operation," in *Advancements in Adaptive Optics*, D. Bonaccini Calia, B. L. Ellerbroek and R. Ragazzoni eds., Proc. SPIE **5490**, 107-117, (2004).
3. J. A.. Stoesz, J.-P. Véran, F. Rigaut, G. Herriot, L. Jolissaint and D. Frenette, "Evaluation of the on-sky performance of Altair," in *Advancements in Adaptive Optics*, D. Bonaccini Calia, B. L. Ellerbroek and R. Ragazzoni eds., Proc. SPIE **5490**, 67–78, (2004).
4. C. Dessenne, P.-Y. Madec, G. Rousset, "Optimization of a predictive controller for closed-loop adaptive optics," Appl. Opt., **37**, 4623–4633, (1998).
5. C. Petit, J.-M. Conan, C. Kulcsár, H.-F. Raynaud, T. Fusco, J. Montri and D. Rabaud,"Optimal Control for Multi-conjugate Adaptive Optics," Comptes Rendus de l'Académie des Science **Physique 6**, 1059–1069, (2005) (http://www.sciencedirect.com/science/journal/16310705).
6. B. Le Roux, J.-M. Conan, C. Kulcsár, H.-F. Raynaud, L. Mugnier and T. Fusco,"Optimal control law for classical and multiconjugate adaptive optics," J. Opt. Soc. Am. A **21**, 1261–1276, (2004).
7. C. Petit, F. Quiros-Pacheco, J.-M. Conan, C. Kulcsár, H.-F. Raynaud, T. Fusco, and G. Rousset, "Kalman Filter based control loop for Adaptive Optics," in *Advancements in Adaptive Optics*, D. Bonaccini Calia, B. L. Ellerbroek and R. Ragazzoni eds., Proc. SPIE **5490**,1414–1425,(2004).
8. C. Kulcsár, H.-F. Raynaud, C. Petit,J.-M. Conan, and P. Viaris de Lesegno, "Optimal control, observers and integrators in adaptive optics," Opt. Express **14**, 7464–7476, (2006)
9. F. Cottet, *Traitement des signaux et acquisition de données* (Dunod,2002).
10. C. Mohtadi., "Bode's integral theorem for discrete-time systems," Proceedings of the IEE **137**, 57–66, (1990).
11. T. Fusco, C. Petit, G. Rousset, J.-F. Sauvage, J.-M. Conan, A. Blanc and J.-L. Beuzit, "Optimization of the pre-compensation of non-common path aberrations for adaptive optics systems," in *Adaptive Optics: Analysis and Methods/Computational Optical Sensing and Imaging/Information Photonics/Signal Recovery and Synthesis Topical Meetings* on CD ROM, OSA electronic proceedings Technical Digest **AWB 2**, Optical Society of America, Charlotte, (2005).

#85269 - $15.00 USD Received 1 Aug 2007; revised 19 Oct 2007; accepted 29 Oct 2007; published 2 Jan 2008

12. C. Dessenne, "Commande modale et prédictive en optique adaptative," Ph. D. thesis, Univ. Paris VII, (1998)
13. C. Petit, "Etude de la commande optimale en Optique Adaptative et Optique Adaptative MultiConjuguée, validation numérique et expérimentale," Ph. D. thesis, Univ. Paris XIII, (2006).
14. R. Paschall and D. Anderson, "Linear Quadratic Gaussian control of a deformable mirror adaptive optics system with time-delayed measurements," Appl. Opt. **32**, 6347–6358, (1993).
15. D. M. Wiberg, C. E. Max, and D. T. Gavel. "A special non-dynamic LQG controller: part I, application to adaptive optics," *Proceedings of the 43th IEEE Conference on Decision and Control*, 3:3333–3338, (2004).
16. D. Looze, "Minimum variance control structure for adaptive optics systems," J. Opt. Soc. Am. A **23**, 603–612 (2006).
17. T. Fusco, G. Rousset, J. -F. Sauvage, C. Petit, J. -L. Beuzit, K. Dohlen, D. Mouillet, J. Charton, M. Nicolle, M. Kasper, P. Baudoz, and P. Puget, "High-order adaptive optics requirements for direct detection of extrasolar planets: Application to the SPHERE instrument," Opt. Express **14** , 7515-7534 (2006).
18. L. A. Poyneer, B. A. Macintosh, and J.-P. Véran, "Fourier transform wavefront control with adaptive prediction of the atmosphere," J. Opt. Soc. Am. A **24**, 2645-2660 (2007).

1. Introduction

Adaptive Optics (AO) allows to perform a real-time correction of the atmospheric turbulence effects on image formation. Nevertheless, AO performance is limited, due to different error terms. One of them is mechanical vibrations which can be of particular concern, as on NAOS [1, 2], where a loss of Strehl Ratio (SR) between 2.5% and 25% could be attributed to vibrations, or on Altair [3], where a 10 to 20 mas rms jitter due to vibrations was estimated. In both cases, these vibrations mainly affected the tip and tilt modes. In both cases, cryo-coolers and electronics were identified as main sources of the vibrations [2]. Telescope and components vibrations (as tip-tilt mirror mount for instance for Altair) were also incriminated. When very high performance is expected, such as in eXtreme AO (XAO), vibrations could then become a burning issue. Vibration filtering could benefit to all AO system but XAO systems require a particular attention on all error terms, especially on tip tilt mode stability. For instance, in the context of the XAO project SPHERE (Spectro-Polarimetric High-contrast Exoplanet REsearch), vibration filtering for tip and tilt modes stabilization is considered.

Passive filtering, performed through smart experimental equipment can reduce vibrations, but fails to filter them entirely. Then, active filtering should be considered, particularly through the control loop. Integrators are not able to filter vibrations specifically, and they may even amplify them depending on the vibrations frequencies. Predictors, such as proposed by Dessenne [4], can filter specific vibrations, but optimality and stability are difficult to ensure. A Linear Quadratic Gaussian (LQG) control law (see [5, 6] and references therein) can provide an optimal (in the sense of residual phase minimal variance) correction of the vibrations [7]. We propose here an experimental validation of this optimal control law. We briefly recall our general LQG control solution and describe the priors used to add vibration filtering. We propose a numerical simulation of the expectable performance on the AO bench with a multiple vibrations pattern. We then focus on experimental validation of vibration filtering in AO. We present the AO bench used for the tests. Then, a single vibration is generated on the bench and filtered with the control law. Results are compared to numerical simulation. We finally discuss the application to the SPHERE project.

2. LQG control and vibration filtering

2.1. LQG control brief overview

The implemented optimal control law is fully described in [7]. The basic assumptions are the following. The DM provides a linear and instantaneous response (no dynamics), constant over a frame period T (zero-order hold) so that the correction phase ϕ_{n-1}^{cor} during time period $[(n-$

#85269 - $15.00 USD Received 1 Aug 2007; revised 19 Oct 2007; accepted 29 Oct 2007; published 2 Jan 2008

$2)T,(n-1)T]$ is

$$\phi_{n-1}^{cor} = \mathbf{N}\mathbf{u}_{n-2}, \tag{1}$$

where $\mathbf{N}$ is the influence matrix. The WFS is linear and integrates the residual phase signal over one frame period. We assume that CCD read-out and slope computation use also one frame period, computation and DM control representing a negligible amount of time. It is thus a two frame period delay system. Phase signal integrated during time interval $[(n-2)T,(n-1)T]$ provides a measurement $\mathbf{y}_n$, which will be used to compute the control voltages $\mathbf{u}_n$ applied during time interval $[nT,(n+1)T]$. Measurement $\mathbf{y}_n$ is defined by:

$$\mathbf{y}_n = \mathbf{D}\left(\phi_{n-1} - \phi_{n-1}^{cor}\right) + \mathbf{w}_n, \tag{2}$$

where $\mathbf{D}$ is a matrix characterizing the WFS, ϕ_{n-1} is the average turbulent signal over time period $[(n-2)T,(n-1)T]$ and $\mathbf{w}_n$ is the measurement noise.

We also define an optimality criterion. For AO applications, a relevant criterion consists in minimizing, over turbulence and WFS noise statistics, the residual phase variance in the pupil defined by:

$$\varepsilon(\mathbf{u}_n) = \left\langle \left\| \phi_{n+1} - \mathbf{N}\mathbf{u}_n \right\|^2 \right\rangle_{turb,noise}. \tag{3}$$

In this context, we have proposed an optimal control law that we briefly recall hereafter. We first exhibit a linear time-invariant state-space model of the system in the form:

$$\mathbf{x}_{n+1} = \mathscr{A}\mathbf{x}_n + \mathscr{B}\mathbf{u}_n + \nu_n, \tag{4}$$

$$\mathbf{y}_n = \mathscr{C}\mathbf{x}_n + \mathbf{w}_n, \tag{5}$$

where $\mathbf{x}_n$ represents the state vector of the system at instant n and gathers all the knowledge needed at instant n to compute the deterministic part of next state $\mathbf{x}_{n+1}$ and output (WFS measurement) $\mathbf{y}_n$. ν_n and $\mathbf{w}_n$ are assumed to be decorrelated zero-mean white Gaussian noises with covariance matrix Σ_ν and $\Sigma_\mathbf{w}$. ν_n represents the stochastic part of state vector $\mathbf{x}_n$, $\mathbf{w}_n$ the measurement noise. A convenient choice of state vector is:

$$\mathbf{x}_n^t = \left(\phi_n^t, \phi_{n-1}^t, \mathbf{u}_{n-1}^t, \mathbf{u}_{n-2}^t\right), \tag{6}$$

where ^{t} stands for transposition. We assume that the dynamics of the turbulent phase (which usually follow a Taylor's hypothesis) can be approximated by a one-order auto-regressive model:

$$\phi_{n+1} = \mathbf{A}_{tur}\phi_n + \nu_n, \tag{7}$$

where ν_n is a zero-mean white Gaussian noise with covariance matrix Σ_ν and $\mathbf{A}_{tur}$ is the matrix defining the dynamical characteristics of the turbulence. Details on computation of $\mathbf{A}_{tur}$ and Σ_ν can be found in [5, 6]. Thus taking into account this model and Eq. 2 then Eq. 4 and Eq. 5 can be written:

$$\mathbf{x}_{n+1} = \begin{pmatrix} \mathbf{A}_{tur} & 0 & 0 & 0 \\ \mathbf{Id} & 0 & 0 & 0 \\ 0 & 0 & 0 & 0 \\ 0 & 0 & \mathbf{Id} & 0 \end{pmatrix} \mathbf{x}_n + \begin{pmatrix} 0 \\ 0 \\ \mathbf{Id} \\ 0 \end{pmatrix} \mathbf{u}_n + \begin{pmatrix} \mathbf{Id} \\ 0 \\ 0 \\ 0 \end{pmatrix} \nu_n, \tag{8}$$

$$\mathbf{y}_n = \mathbf{D}\begin{pmatrix} 0 & \mathbf{Id} & 0 & -\mathbf{N} \end{pmatrix} \mathbf{x}_n + \mathbf{w}_n. \tag{9}$$

Based on the separation principle, the control issue is then split into first an optimal estimation of the incoming phase and then phase correction [8]. Estimation is based on a Kalman

#85269 - $15.00 USD Received 1 Aug 2007; revised 19 Oct 2007; accepted 29 Oct 2007; published 2 Jan 2008

filter and provides a reconstruction of the phase on a truncated Zernike basis of N modes. It realizes a temporal prediction accounting for time delay. More precisely, optimal estimation and prediction of the turbulence is provided by:

$$\hat{\mathbf{x}}_{n+1/n} = \mathscr{A}\hat{\mathbf{x}}_{n/n-1} + \mathscr{B}\mathbf{u}_n + \mathscr{L}_n(\mathbf{y}_n - \mathscr{C}\hat{\mathbf{x}}_{n/n-1}). \tag{10}$$

Of course, for a structure such as Eq. (8) and Eq. (9), only the first two coordinates of $\mathbf{x}$ are to be estimated (that means $2 \times N$ if N is the number of modes on which the phase is expressed), the voltages being known. Eq. (10), when detailed for each coordinate of $\hat{\mathbf{x}}_{n+1/n}$ simply gathers estimations of ϕ_{n+1} and ϕ_n plus useless equations consisting in buffering voltages. The voltages can thus be discarded from the state vector for computation efficiency, but their presence remains interesting for comprehension. The Kalman optimal observer corresponds to a particular value of the gain $\mathscr{L}_n$ given by

$$\mathscr{L}_n = \mathscr{A}\Sigma_{n/n-1}\mathscr{C}^t(\mathscr{C}\Sigma_{n/n-1}\mathscr{C}^t + \Sigma_w)^{-1}, \tag{11}$$

where $\Sigma_{n/n-1}$ is the covariance matrix of the state estimation error and is obtained by solving the following Riccati matrix equation:

$$\Sigma_{n+1/n} = \mathscr{A}\Sigma_{n/n-1}\mathscr{A}^t + \Sigma_v - \mathscr{A}\Sigma_{n/n-1}\mathscr{C}^t(\mathscr{C}\Sigma_{n/n-1}\mathscr{C}^t + \Sigma_w)^{-1}\mathscr{C}\Sigma_{n/n-1}\mathscr{A}^t. \tag{12}$$

This equation does not depend on measurement and can be therefore computed off-line, or replaced by its constant asymptotic solution $\mathscr{L}_\infty$ (by letting $\Sigma_{n+1/n}$ in Eq. (12) converge to its asymptotical value) with no loss of optimality, as in [6].

Correction is then deduced thanks to a classic least-square projection of the predicted turbulent phase onto the DM modes. The state feedback form is then:

$$\mathbf{u}_n = \mathbf{K}\hat{\mathbf{x}}_{n+1/n}, \tag{13}$$

where $\mathbf{K} = (P, 0, 0, 0)$ and $P = (\mathbf{N}^t\mathbf{N})^{-1}\mathbf{N}^t$. Note that the classical form $\mathbf{u}_n = \mathbf{K}\hat{\mathbf{x}}_{n/n}$ is obtained for a state vector defined as $\mathbf{x}_n^t = \left(\phi_{n+1}^t, \phi_n^t, \phi_{n-1}^t, \mathbf{u}_{n-1}^t, \mathbf{u}_{n-2}^t\right)$ and $\mathbf{K} = (0, P, 0, 0, 0)$ as in [6], which gives exactly the same result. This control law, called standard LQG control henceforth, has been already thoroughly simulated and experimentally validated in classic AO, off-axis AO, and MCAO [5].

2.2. Vibration filtering

We now assume that a phase perturbation ϕ_n^{vib} due to vibrations is added to the incoming turbulent phase, so that the global phase can be noted:

$$\phi_n^{glob} = \phi_n + \phi_n^{vib}. \tag{14}$$

Additive vibrations are straightforwardly included as perturbations in the state vector and estimated just as the turbulence. We only need to modify our models to describe explicitly the impact of vibrations on the phase. Estimation then takes additive priors on this new perturbative term into account, but the overall structure of the control law is identical. For simplicity, we first assume the existence of one vibration on a particular mode of the phase, so that we deal, as a first step, with a scalar problem. We need to define a model of this perturbation, in a discrete-time domain.

Considering first a continuous-time description, a dampened oscillatory signal ϕ generated by a forcing function ξ at the pulsation $\omega_0 = 2\pi f_{vib}$ (natural frequency f_{vib}) is commonly described by the second-order differential equation:

$$\ddot{\phi} + 2K\omega_0\dot{\phi} + {\omega_0}^2\phi = C{\omega_0}^2\xi, \tag{15}$$

#85269 - $15.00 USD Received 1 Aug 2007; revised 19 Oct 2007; accepted 29 Oct 2007; published 2 Jan 2008

where C is the static gain and K the damping coefficient (we consider the dampened case where $0 < K < 1$). Considering a continuous-time causal signal, a Laplace transform of the previous equation leads to:

$$\tilde{\phi}(p) = H(p)\tilde{\xi}(p), \tag{16}$$

where $H(p)$ is the transfer between $\tilde{\xi}$ and $\tilde{\phi}$:

$$H(p) = \frac{C{\omega_0}^2}{p^2 + 2K\omega_0 p + {\omega_0}^2}. \tag{17}$$

The point is now to provide a discrete-time representation of $H(p)$ so as to propose a linear discrete-time representation of the evolution of the discrete-time oscillatory signal in an Auto-Regressive Moving Average (ARMA) form (ratio of polynoms in z). A common approach is to consider the discrete-time signals, obtained through zero-order hold sampling (with period T):

$$\phi_n = \phi(nT),\ \xi_n = \xi(nT). \tag{18}$$

These signals being causal, their Z transform $\tilde{\phi}(z)$ et $\tilde{\xi}(z)$ are linked by:

$$\tilde{\phi}(z) = H(z)\tilde{\xi}(z). \tag{19}$$

$H(z)$ is rigorously obtained from $H(p)$ using the relation:

$$z = e^{pT}. \tag{20}$$

This relation leads however to a complex form of $H(z)$ (including the logarithm of z), not suited for an ARMA representation. Various classical methods of signal processing allow nevertheless to approximate $H(z)$ in an ARMA representation. It appears that an adapted transformation [9] is convenient, as it maintains the poles of the transfer, and in this particular case it also maintains its impulsional and indicial responses. This transformation is obtained replacing $\frac{1}{p-p_i}$ (where p_i are the poles of the transfer function H) by $T\frac{1}{1-e^{p_i T}z^{-1}}$ and leads to:

$$H(z) = C{\omega_0}^2 T \frac{1}{1 - 2e^{-K\omega_0 T}\cos(\omega_0 T\sqrt{1-K^2})z^{-1} + e^{-2K\omega_0 T}z^{-2}}. \tag{21}$$

Considering the perturbation ϕ_n^{vib}, this leads to the following second-order Auto-Regressive (AR2) model:

$$\phi_n^{vib} = a_1\phi_{n-1}^{vib} + a_2\phi_{n-2}^{vib} + \xi_n, \tag{22}$$

where the coefficients a_1, a_2 are defined by

$$a_1 = 2e^{-K\omega_0 T}\cos(\omega_0 T\sqrt{1-K^2}),\ a_2 = -e^{-2K\omega_0 T}. \tag{23}$$

The damping coefficient K is related to the vibration bandwidth. The forcing function ξ_n is in general unknown and can be modeled consequently as a Gaussian white noise of variance σ_ξ^2. For a given (ω_0, K), the power of the vibration ϕ_n^{vib} is proportional to σ_ξ^2. This model defines our priors on the vibration from which a vibration filtering LQG control is derived. Note that this process allows to filter any vibration which frequency is lower than half the sampling frequency.

The state vector can then take the following structure:

$$\mathbf{x}_n^t = \left(\phi_n^{vib\,t}, \phi_{n-1}^{vib\ \ t}, \phi_n^t, \phi_{n-1}^t, \mathbf{u}_{n-1}^t, \mathbf{u}_{n-2}^t\right). \tag{24}$$

#85269 - $15.00 USD Received 1 Aug 2007; revised 19 Oct 2007; accepted 29 Oct 2007; published 2 Jan 2008

The measurement equation Eq. (2) now takes into account the global phase so that:

$$\mathbf{y}_n = \mathbf{D}\left(\phi_{n-1}^{glob} - \phi_{n-1}^{cor}\right) + \mathbf{w}_n. \tag{25}$$

The various matrices of the state space model in Eq. (4) and Eq. (5) are easily modified accordingly and the estimation of the vibration and turbulence is still provided by an equation of the form of Eq. (10). Correction is also performed similarly, by projecting both the turbulence and the vibration onto the DM. Note that another application of this approach could be to estimate both vibration and turbulence but to correct only turbulence. This approach would be useful when vibrations affect the WFS arm and not the imaging arm.

We have considered here the estimation and correction of one vibration on one mode, but we could account similarly for p vibrations on M different modes of the phase, dealing with each mode separately. Assuming vibrations are not coupled, this leads to the estimation of $2 \times p \times M$ components in addition to the $2 \times N$ turbulent components but generally $p \times M << N$. We assume that calibrations or a proper identification process provide the parameters $\omega_0, K, \sigma_\xi^2$ for each vibration on each phase mode.

3. Numerical simulation

As a first illustration, we have numerically simulated an AO case with an end-to-end simulator. In the prospect of experimental validation described in Sect 4, the simulator reproduces faithfully our AO bench (see Sect. 4.1) and its components: the DM is described by an experimental influence matrix, the WFS model is based on a geometric model of the Shack-Hartmann WFS, the one-layer turbulence has Kolmogorov statistics and is translated across the pupil (Taylor hypothesis). These models are fitted to the experiment described in Sect 4 thanks to calibrations. The sampling frequency is set, as in the experiment, to 60 Hz. Three vibrations have been added to the incoming Kolmogorov turbulence: two quasi-pure harmonic vibrations ($K_{1,2} = 10^{-5}$) at 6 Hz and 15 Hz with $(\sigma_\xi^2)_{1,2} = 10^{-10}\text{rad}^2$, and a vibration with wider bandwidth ($K_3 = 3\,10^{-2}$) centered at 8 Hz with $(\sigma_\xi^2)_3 = 10^{-3}\text{rad}^2$. Characteristics of these vibrations have been chosen first to propose both narrow and broad-band vibrations, then to provide distinct vibrations distributed beyond the AO loop bandwidth. For simplicity, we assume that these vibrations only affect the tip and tilt modes. Such vibrations significantly decrease the AO loop performance. When simulating a closed-loop AO with either an integrator or a standard LQG control (turbulence estimated on $N = 120$ modes), the SR decreases from 91% down to 76%. Indeed these standard control laws do not filter out the vibrations (which frequencies are above the AO loop bandwidth) but rather amplify them. Now we consider a vibration filtering LQG control. Priors for vibration filtering match the three vibrations characteristics and $2p \times M = 12$ additional components are estimated. Vibration filtering allows then to increase the SR back up to 89%. This performance can also be seen on temporal spectra. As the vibrations only affect the tip and tilt modes, we focus on the spatially averaged x and y slopes of the WFS and compare their Power Spectral Density (PSD), estimated thanks to periodograms, in open-loop $PSD_{ol}^{x,y}(\nu)$ and closed-loop $PSD_{cl}^{x,y}(\nu)$, for the LQG control, with or without vibration filtering. We can then evaluate the gain of the slope transfer function $T_{x,y}(\nu)$ using:

$$|T_{x,y}(\nu)| = \frac{\sqrt{PSD_{cl}^{x,y}(\nu)}}{\sqrt{PSD_{ol}^{x,y}(\nu)}}. \tag{26}$$

This function describes the effect of the AO loop on turbulence plus vibration. Fig. 1 presents the $|T_x(\nu)|$ function for the LQG control, with or without vibration filtering. The overall structure of this transfer is complex and related to the LQG control properties, but it clearly shows the

#85269 - $15.00 USD Received 1 Aug 2007; revised 19 Oct 2007; accepted 29 Oct 2007; published 2 Jan 2008

vibrations damping introduced by the adapted control law. The LQG control performs the best compromise between the correction of the different components (turbulence and vibrations). This compromise is related to the power and spectrum of each component. Differences appear

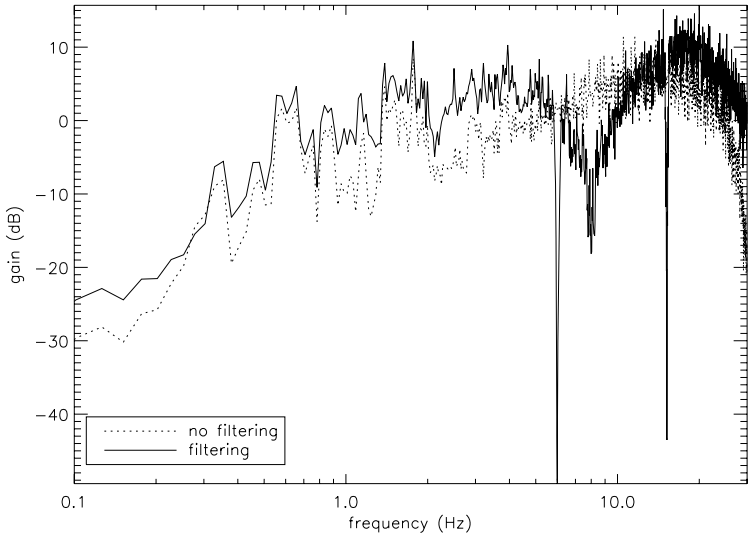

Fig. 1. Numerical simulation of three vibrations filtering (pure at 6,15 Hz, large at 8 Hz). Transfer $|T_x(\nu)|$ of the x average slope is plotted for standard and vibration filtering LQG control law.

between the two PSDs in particular at very low frequencies. This is due first to computation of PSD over a finite time series. Averaged periodograms could provide more accurate results but at the expense of spectral resolution. Moreover, Bode's integral theorem [10] justifies that vibrations filtering leads to a loss of turbulence correction (the normalized integral of the PSD is always equal to 1 whatever the stabilizing controller) and thus differences between PSDs.

4. Experimental validation

4.1. Experimental set-up description

Tests of the LQG control for vibration filtering have been performed thanks to the AO test bench developed by ONERA. It is composed of a turbulence generator, a telescope simulator, the AO system and an imaging camera. The source is a LASER diode working at $\lambda = 633$ nm. The turbulence generator is based on a phase screen mirror mounted on a rotating stage to reproduce wind effects (wind speed V is scaled to reproduce an equivalent $V/D \simeq 0,28$ Hz, D being the pupil diameter), and placed in a collimated beam. The phase screen reproduces a Kolmogorov turbulence which strength corresponds to $D/r_0 \simeq 2.8$ at 633 nm. It is weak but does not restrict the demonstration provided that the power of the vibration is selected accordingly. Wavefront correction is based on a Tip Tilt Mirror (TTM) and a 9×9 actuator DM (69 valid actuators). The Shack-Hartmann WFS is composed of a 8×8 lenslet array (52 sub-pupils used) and a CCD camera. The sampling frequency $f_e = 1/T$ is set to 60 Hz. The overall loop has a two frame delay. A specific phase diversity calibration [11] allows to reach an internal Strehl Ratio (SR) (without turbulence) of 95%@633 nm. A standard integrator and a LQG control law [5] can both be used for AO correction of the turbulence. The integrator gain is optimized thanks to Dessenne procedure [12], but as the signal to noise ratio is very high, it can be set to a

#85269 - $15.00 USD Received 1 Aug 2007; revised 19 Oct 2007; accepted 29 Oct 2007; published 2 Jan 2008

global value of 0.5 without loss of performance. When dealing with the turbulence and without vibrations, both control laws lead to 91% SR (estimated on long exposure images), in these rather favorable conditions.

So as to validate vibration filtering on this AO bench, we need a stable vibration. We have thus used a seismic vibration generator to move the optical bench in an horizontal plane with a quasi pure sinusoidal mechanical oscillation. Figure 2 shows a picture of the set-up.

Fig. 2. Picture of the experimental set-up for vibration filtering validation. The AO bench is on the right, under its baffling. The seismic vibration generator is in the middle of the picture, placed on its stage and against the AO bench (cylindrical black component).

4.2. Vibration characterizations

We now need to evaluate the impact of the seismic vibrator on the bench. Calibrations, based on recordings and analysis of WFS data, indicate that the bench has a linear response to the excitation, leading to a global oscillation of the system at the same frequency as the excitation. The induced vibration has a good stability and purity, as $f_{vib}/\Delta f > 2500$, where Δf is the Full Width at Half Max (FWHM) of the vibration. The peak-valley amplitude of the vibration is $A = 0.24\ \lambda/D$. This vibration mainly affects the tip and tilt modes, and so the x and y average slope measurements. Closing the AO loop with standard control laws (either integrator or LQG without specification of vibration filtering) leads to a drop of the long exposure SR down to 86% (compared to 91% without vibrations), due to image jitter. Meanwhile, x and y average slopes measured on the WFS show an increased variance and a resonance peak at frequency f_{vib}. In terms of root-mean-square tilt (x axis) expressed in fraction of λ/D, the vibration leads to an increase from 0.05 up to 0.10. On Fig. 3, the Cumulated Temporal PSD (CTPSD) of the x average slope, in closed-loop, shows a steep step due to the vibration. Indeed with the selected frequency $f_{vib} = 15.2$ Hz, the vibration is not damped, and even amplified by standard control laws. Loss of SR and average slope variance increase are consistent, proving that vibration is

#85269 - $15.00 USD Received 1 Aug 2007; revised 19 Oct 2007; accepted 29 Oct 2007; published 2 Jan 2008

common to both imaging and WFS arms and should be estimated and corrected. Optimization of the integrator gain is useless as the power of the vibration is too weak compared to the turbulence power. Such a scenario is rather realistic compared to the vibration effects measured on systems like NAOS [1] even if the vibration introduced may seem weaker (only a 5% loss of SR). But we are limited by the seismic vibrator, used at full power to shake the AO bench.

We now consider implementing vibration filtering with LQG control. We have stressed that the tip and tilt modes mainly suffer from the vibration. Vibration filtering is thus applied only on these two modes, leading to a negligible computational cost increase ($N = 120$, $p \times M = 2$). The parameters of the AR2 model of the vibration are estimated thanks to open-loop measurements and CTPSDs, leading to $f_{vib} = 15.2$ Hz (position of step induced by vibration in CTPSD), $K = 10^{-4}$ (computed from FWHM on PSD) and $\sigma_\xi^2 = 5,4\ 10^{-6}\text{rad}^2$ (deduced from step amplitude in CTPSD).

4.3. Vibration filtering results

When closing the AO loop with vibration filtering LQG control, the vibration is strongly attenuated. The SR increases up to 90%, close to the vibration free performance of the standard control laws (91%). In terms of root-mean-square tilt this corresponds to a significant drop down to $0.06\ \lambda/D$. Comparison of the CTPSD of the *x* average slope with or without vibration for standard control and for vibration filtering LQG control is given in Fig. 3. It shows that the steep step due to the vibration is almost completely damped. In fact, a slight residual step is still visible since a compromise (Bode's theorem) is made between the filtering of the vibration and the correction of the turbulence. Small differences can be seen on this figure between the dif-

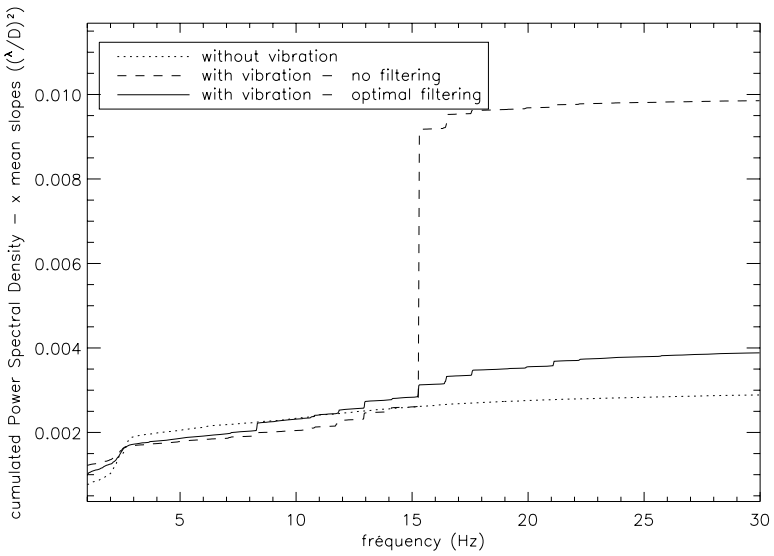

Fig. 3. Experimental CTPSD of the *x* average slope for a LQG control law, without vibration (dotted line), with vibration and no specific filtering (dashed), and with vibration filtering (solid). Experimental error bound is lower than $\pm 2.5\ 10^{-4}(\lambda/D)^2$.

ferent CTPSD in particular at low frequencies. They are mainly due to experimental variability, all the more as the AO bench is not mechanically stabilized. Note that experimental error bound is lower than $\pm 2.5\ 10^{-4}(\lambda/D)^2$.

We provide on Fig. 4 the *x* average slope transfer functions as defined in Eq. (26) for ei-

#85269 - $15.00 USD Received 1 Aug 2007; revised 19 Oct 2007; accepted 29 Oct 2007; published 2 Jan 2008

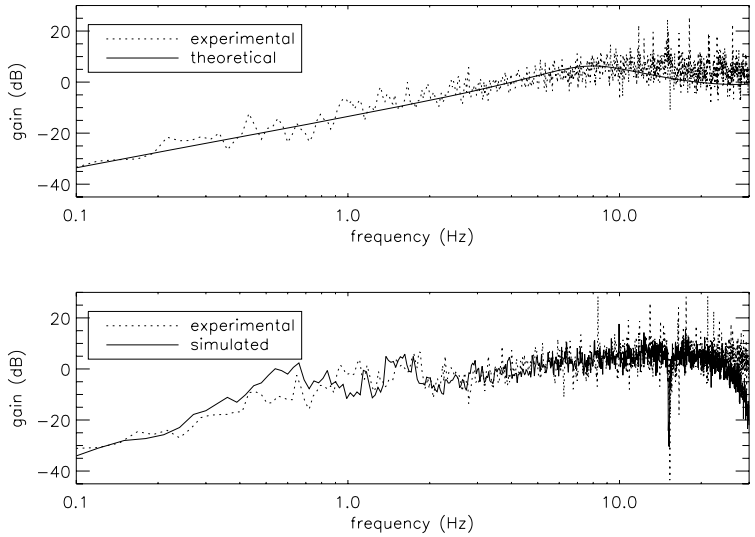

Fig. 4. Comparison of the experimental *x* average slope transfer. Top is obtained with integrator (dotted) and compared to theory (solid). Bottom is obtained with vibration filtering LQG control (dotted) and compared to numerical simulation (solid).

ther the integrator (compared to theory), or the LQG control (compared to simulation). As for the integrator, a good agreement is found between experimental transfer and theory. A logical strong damping is observed on the LQG control transfer at f_{vib}. The peculiar low frequency behavior on the experimental PSD is consistent with simulation results. It is characteristic of the LQG control, and so is the high frequency (close to $f_e/2$) loss of gain of the simulated PSD. This loss of gain is not observed on experimental data due to high frequency defects of the experimental set-up not accounted for in the simulations. Finally, experimental curves of Fig. 4 show that some small peaks appear between 8 Hz and 12 Hz, due to non stationary vibrations present on the bench and related to the lab environment (building vibrations etc). Performance in the various conditions are summarized in table 1.

	integrator	standard LQG	LQG + vibration filtering
no vibration	91	91	91
vibration	86	86	90

Table 1. Performance in terms of Strehl Ratio (SR) for the various control laws, in presence or not of vibration. SR are given with a $\pm 0.5\%$ error bar. Error on SR evaluation is statistically estimated on a large number of measurements and error bar corresponds to $\pm$ the root mean square.

Note in table 1 (last column) that applying LQG control with vibration filtering when no vibration exists on the bench does not degrade the system performance. This result is confirmed by numerical simulations.

5. Discussion

We have not addressed here the problem of robustness. First, the good results obtained in this experimental validation, despite unavoidable model errors, indicate a good robustness of the

#85269 - $15.00 USD Received 1 Aug 2007; revised 19 Oct 2007; accepted 29 Oct 2007; published 2 Jan 2008

overall control law. Moreover, irrespective of the particular choice of controller structure and/or design method, vibration filtering ultimately boils down to lowering the controller gain for the frequencies that need to be filtered out. Obviously, lowering this gain over too large a frequency range is bound to degrade overall performance. Thus, a delicate balance needs to be achieved between robustness (measured by the width of the frequency band where filtering is effective) and performance. In the LQG approach presented in this paper, this engineering trade-off is embodied for instance in the choice of the dampening coefficient K, a low value of which results in a controller which effectively filters out vibrations only in a narrow frequency band around the vibration frequency. Nevertheless the impact of model parameters modification and the resulting engineering trade-off have not been evaluated so far. This issue is currently under investigation.

Indeed, these promising results have led us to consider a LQG control for the tip and tilt modes correction for the SPHERE project [17], the higher order modes being corrected thanks to a classic optimized modal gain integrator. It allows correcting both turbulence and vibrations on tip and tilt modes, which is of particular concern for coronagraphic applications, with no significant increase of the computational cost. This dual control leads to particular issues of control loops decoupling to avoid cross-talk between the tip-tilt and higher order modes correction. Good results have been obtained here for these first numerical and experimental application of LQG approach. Still, to deal with robustness issues, the control procedure should be based on a real-time identification procedure of the vibration parameters for a regular update of the LQG control.

6. Conclusion

We have proposed in this paper to include vibration filtering in a LQG control dedicated to AO closed-loop correction. First experimental validation of this scheme has been successfully performed. It demonstrates the significant improvement of performance brought by correction of such components. Multiple vibrations can also be filtered out as shown numerically. Robustness issues are still under investigation, but most AO systems and more particularly XAO systems could benefit from this control solution.

Previous works on optimal control in AO ([5, 6, 14, 15, 16, 18]) have underlined the interest of LQG control to optimize the correction in tomographic AO, based on complex wave-front sensing and correction configurations. Recent studies based on experimental and numerical validations have for instance demonstrated the gain brought by LQG control in MultiConjugate AO and Laser Tomographic AO (LTAO) ([5, 13]). The vibration filtering approach proposed here has the advantage of being developed in the same LQG framework, hence adding an additional feature that could also easily benefit to the control of such complex systems.

#85269 - $15.00 USD Received 1 Aug 2007; revised 19 Oct 2007; accepted 29 Oct 2007; published 2 Jan 2008